

## Research Paper

# ESCO2 promotes the proliferation of hepatocellular carcinoma through the PI3K/AKT/ mTOR signaling pathway

Dapeng Chen<sup>1†</sup>, Yue Huang<sup>2†</sup>, Weixin Zhang<sup>1</sup>, Youcheng Zhang<sup>1</sup>, Yi Bai<sup>3</sup>, Yamin Zhang<sup>3✉</sup>

1. First Central Hospital of Tianjin Medical University, Tianjin Medical University, Tianjin 300070, China.
2. Daping Hospital, Army Medical University, Chongqing 400000, China.
3. Department of Hepatobiliary Surgery, Tianjin First Central Hospital, Tianjin 300192, China.

†These authors contributed equally to this work.

✉ Corresponding author: Yamin Zhang, zhangyamin@nankai.edu.cn.

© The author(s). This is an open access article distributed under the terms of the Creative Commons Attribution License (<https://creativecommons.org/licenses/by/4.0/>). See <https://ivyspring.com/terms> for full terms and conditions.

Received: 2025.02.13; Accepted: 2025.05.27; Published: 2025.06.23

## Abstract

**Background:** Establishment of sister chromatid cohesion N-Acetyltransferase 2 (ESCO2) is a gene implicated in the establishment of sister chromatid cohesion (SCC) and cell proliferation. We aimed to explore how ESCO2 affects the proliferation of hepatocellular carcinoma (HCC).

**Methods:** We analyzed ESCO2 expression levels and their association with clinical prognosis using the TCGA, HCCDB, and ICGC databases. Bioinformatics methods were employed to investigate potential regulatory pathways involving ESCO2. CCK-8 assays, colony formation assays, and flow cytometry were used to examine the impact of ESCO2 knockdown on the malignant biological behavior of HCC cells. Western blotting was utilized to identify the specific regulatory mechanism of ESCO2.

**Results:** ESCO2 was significantly upregulated in HCC tissues and correlated with a worse prognosis. Bioinformatics analysis revealed that ESCO2 regulated pathways related to the cell cycle and cell proliferation. Furthermore, knockdown of ESCO2 significantly inhibited HCC cell proliferation both *in vivo* and *in vitro*. Most importantly, ESCO2 stimulated the PI3K/AKT/mTOR pathway, which ultimately accelerated the cell cycle and inhibited apoptosis, promoting HCC progression.

**Conclusion:** The present study elucidated the mechanism by which ESCO2 regulates HCC proliferation: ESCO2 promotes HCC proliferation by accelerating the cell cycle and inhibiting apoptosis via the PI3K/AKT/mTOR signaling pathway.

Keywords: Hepatocellular carcinoma; ESCO2; Cell cycle; Apoptosis; PI3K/ AKT/ mTOR signaling pathway

## Background

Liver cancer, specifically hepatocellular carcinoma (HCC), is one of the most prevalent solid cancers worldwide, posing a significant global health burden [1, 2]. With a relatively low 5-year survival rate of approximately 18%, HCC remains one of the deadliest malignancies [3]. The majority of HCC patients are diagnosed at an advanced stage, limiting treatment options to local and systemic therapies, excluding surgery or liver transplantation. Currently, systemic therapy is the standard approach for treating advanced HCC in clinical settings [4], ranging from

single-agent targeted therapies (sorafenib or lenvatinib) to combinations of immune checkpoint inhibitors and targeted therapies (atezolizumab plus bevacizumab). Despite significant advancements in systemic therapy, advanced HCC remains a challenging and often fatal disease, given that only a minority of patients achieve durable clinical benefits [5]. The carcinogenesis of HCC is now understood to be a complex process, and research has shown that abnormal proliferation is a crucial driver of HCC development [6]. Investigating the molecular

mechanisms that regulate HCC proliferation will enhance our understanding of its pathogenesis and identify potential therapeutic targets, which may improve patient outcomes in the future.

Establishment of sister chromatid cohesion N-Acetyltransferase 2 (*ESCO2*) is a novel gene implicated in cell proliferation. It belongs to the family of histone acetyltransferases (HATs) that regulate numerous vital biological processes [7]. The *ESCO2* protein is essential for establishing sister chromatid cohesion (SCC) during the S phase of the cell cycle [8]. Sister chromatid cohesion facilitates accurate chromosome segregation, which is crucial for cell cycle progression [9]. Previous studies on *ESCO2* have revealed that human *ESCO2* mutations result in Roberts syndrome, an inherited developmental disorder characterized by SCC defects and aberrant transcriptional acetylation [10]. According to previous research, *ESCO2* is linked to the development of several malignancies, making it a potential biomarker and therapeutic target. *ESCO2* is significantly upregulated in kidney cancer tissues, and *ESCO2* knockdown inhibits cancer cell growth, invasion, and migration by regulating the AKT/mTOR pathway [11]. Zhu et al. also demonstrated that *ESCO2* could promote lung adenocarcinoma (LUAD) cell proliferation and metabolic reprogramming of metastasis *in vitro* and *in vivo* [12]. However, *ESCO2* has been shown to inhibit cancer metastasis in colorectal cancer by reducing MMP2 expression [13]. To date, no studies have explored the expression of *ESCO2* and its functional role in HCC.

In this study, multi-source high-throughput data analysis revealed that *ESCO2* was significantly upregulated in HCC tissues. Furthermore, HCC patients with high *ESCO2* expression exhibited poorer prognoses. Additionally, *ESCO2* knockdown markedly suppressed HCC cell proliferation both *in vivo* and *in vitro*. Notably, *ESCO2* could promote the PI3K/AKT/mTOR pathway, accelerating the cell cycle and inhibiting apoptosis, thereby increasing HCC growth. Therefore, *ESCO2* represents a potential molecular target for HCC.

## 2. Methods and Materials

### 2.1 Data preparation and differential expression analysis

The bulk mRNA sequencing profiles of liver hepatocellular carcinoma (LIHC) and normal liver tissue samples were acquired from the International Cancer Genome Consortium (ICGC, <https://dcc.icgc.org/>) and The Cancer Genome Atlas (TCGA, <https://portal.gdc.cancer.gov/>) database. Concurrently, the single-cell RNA sequencing matrix,

encompassing 10 tumor tissues and 7 normal tissues, was obtained from GSE149614 (<https://www.ncbi.nlm.nih.gov/geo/>) [14]. Spatial transcriptome sequencing data (HRA000437) [15] was accessed from the Genome Sequence Archive (GSA, <https://ngdc.cncb.ac.cn/gsa/>). The spatial transcriptomics data of HCC leading-edge sections were selected for further analysis.

TCGA database was initially used to assess the differential expression of *ESCO2* mRNA between tumor and normal samples, which contains 374 tumor tissues and 50 adjacent normal tissues. Additionally, the HCCDB database [16], a comprehensive platform (<http://lifeome.net/database/hccdb/home.html>) incorporating all HCC mRNA sequencing data, was utilized to examine *ESCO2* expression levels. In addition, we employed the Seurat R package to process spatial transcriptomics data and performed log-normalization to standardize the data. The expression level and distribution of *ESCO2* were visualized on leading-edge sections using Seurat's SpatialFeaturePlot function. Finally, four pairs of HCC and adjacent non-malignant tissue samples were collected from Tianjin First Central Hospital. None of them received preoperative chemotherapy or radiotherapy. All patients provided informed consent for the use of surgical material for academic research and publication. All methods were approved by the Institutional Review Board and the Medical Ethics Committee of Tianjin First Central Hospital.

### 2.2 Survival analysis and functional enrichment analysis

We first excluded samples without follow-up data or with a follow-up time of 0. We then performed survival analysis using the survival R package. Kaplan-Meier survival curves were modeled using the "survfit" function. The optimal cutoff point for gene expression was determined using the "surv\_cutpoint" function from the survminer R package. Patients were then divided into two groups based on the optimal cutoff point, and Kaplan-Meier survival curves were modeled for each group. Additionally, we calculated the correlation between clinical data (tumor size, stage, grade, and survival status) and *ESCO2* expression levels. The clinical parameters and corresponding *ESCO2* expression values of the enrolled patients are listed in Table S2.

To explore the biological functions of *ESCO2* in HCC, individuals in the LIHC cohort were divided into *ESCO2*-high and *ESCO2*-low subsets based on the median *ESCO2* expression value. Gene Set Enrichment Analysis (GSEA) was performed to determine whether predefined gene sets exhibited significant differences between the two subgroups.

Two HCC RNA-seq datasets, TCGA-LIHC and ICGC, were utilized to identify ESCO2-related regulatory genes. In each dataset, individuals were divided into ESCO2-high and ESCO2-low subsets based on the median ESCO2 expression value. Subsequently, a differential expression analysis was conducted to identify differentially expressed genes (DEGs) between the ESCO2-high and ESCO2-low subgroups ( $p < 0.05$ ,  $\log FC \geq 1$ ). The association between ESCO2 and these DEGs was then determined using Spearman's correlation analysis in both datasets ( $p < 0.05$ , correlation coefficient  $\geq 0.3$ ). Intersecting genes from these closely related gene sets were identified as ESCO2-related regulatory genes. Finally, the functional roles of these regulatory genes were elucidated using the Metascape online platform.

### 2.3 Single-cell analysis

All cells were filtered through quality control, retaining cells with RNA counts ranging from 200 to 7000 and mitochondrial gene expression percentages less than 5%. Data were normalized using the "LogNormalize" approach with a scale factor of 10,000. Seurat's CellCycle Scoring function was employed to determine each cell's cell cycle score. The influence of UMI counts and mitochondrial content was regressed using Seurat's ScaleData function. Subsequently, batch effects were eliminated using the Harmony R package. The top 30 principal components and the top 2000 variable genes were selected for cell clustering and uniform manifold approximation and projection (UMAP) visualization. Canonical marker genes identified in previous studies were utilized to annotate cell types. DEGs were identified using the FindMarkers function. Gene Ontology (GO) and Kyoto Encyclopedia of Genes and Genomes (KEGG) pathway enrichment analysis for DEGs was performed using clusterProfiler R packages [17]. Additionally, Gene Set Variation Analysis (GSVA) was employed to assess the expression scores of 50 hallmark pathways among cell clusters.

### 2.4 Cell culture and transfection

Huh7 and MHCC97H cell lines were obtained from ICell Bioscience Inc. (Shanghai, China). All hepatoma cell lines were cultured in DMEM medium (Gibco BRL Life Technologies Inc., USA) supplemented with 10% fetal bovine serum (FBS) (Gibco BRL Life Technologies Inc., USA) and 1% penicillin-streptomycin (HyClone, CA, USA) at 37°C. To ensure effective suppression of ESCO2 expression, two independent small interfering RNAs (siRNAs) were designed. The siRNAs were ordered from GenePharma, and their sequences are listed in Table S1. Hepatoma cell lines were transfected with siRNA

using a transfection reagent (Thermo Fisher Scientific, United States) according to the manufacturer's protocol when cells reached 70-80% confluence in the culture plate.

The shRNA constructs targeting ESCO2 and negative controls were obtained from GenePharma. Huh7 and MHCC97H cell lines were infected with lentiviral particles expressing the ESCO2-targeting shRNA, following the manufacturer's protocol. Stable transfectants were selected using 10  $\mu\text{g/mL}$  puromycin (Sigma-Aldrich, St. Louis, MO, USA). The sequence of the shRNA targeting ESCO2 was 5'-GCAAATCAAGGCTCACCAT-3'.

### 2.5 RT-qPCR and western blotting

The cells were harvested for RNA and protein extraction after 48 and 72 hours of siRNA transfection, respectively. Total RNA was extracted using TRIzol reagent (Invitrogen). RNA quantification was performed using the One-Step SYBR PrimeScript RT-PCR kit (Takara, Japan), and cDNA was synthesized using the cDNA Reverse Transcription Kit. ESCO2 expression was normalized to GAPDH and calculated using the  $2^{-\Delta\Delta C_t}$  method. The primers used are listed in Table S1 (Sangon Biotech).

Cells were harvested and incubated with RIPA lysis buffer (Thermo Fisher Scientific, USA) supplemented with a protease inhibitor cocktail (Roche, Switzerland) on ice for 30 minutes to extract cellular proteins. Tumor tissue proteins were isolated using the Tissue Protein Extraction Reagent (Thermo Fisher Scientific, USA) according to the manufacturer's protocol. Protein concentration was measured using the BCA assay (Thermo Fisher Scientific, USA). Equivalent amounts of total protein from each group were separated by sodium dodecyl sulfate-polyacrylamide gel electrophoresis (SDS-PAGE) and transferred to a nitrocellulose membrane. After blocking with 5% non-fat milk for 1 hour, primary and secondary antibodies (Table S1) were applied according to standard Western blotting procedures. Protein bands were visualized using SuperKine™ West Femto Maximum Sensitivity Substrate (Abbkine) and detected with an imaging system (Tanon, Shanghai, China). The grayscale intensity of protein bands was quantified using ImageJ software. All antibodies used are listed in Table S1.

### 2.6 Cell proliferation and colony formation assay

For the CCK-8 experiment, 2000 cells were seeded into a 96-well plate, transfected, and cultured for a specified duration. Each well received 10  $\mu\text{L}$  of CCK-8 reagent. After a 2-hour incubation, the

absorbance at 450 nm was measured. To evaluate colony formation capacity, 1000 cells were seeded into 6-well plates and cultured for 12 days. Cells were fixed and stained when visible colonies appeared. The number of colonies in each well was then counted.

## 2.7 Ethynyl-2-Deoxyuridine (EdU) incorporation assay

Cell proliferation was assessed using an EdU imaging analysis kit (Abbkine, Wuhan, China). 50,000 cells were seeded per 15 mm glass-bottom culture dish and transfected. Following transfection, the culture medium was removed, and a suitable volume of EdU (ApexBio Technology LLC) was added according to the manufacturer's instructions. Cells were incubated for 2 hours, then fixed and stained with DAPI (Sigma-Aldrich, USA) for nuclear counterstaining. The percentage of EdU-positive cells (red) was determined using a fluorescence microscope (Nikon, Tokyo, Japan).

## 2.8 Flow cytometry related to cell cycle and apoptosis

Both normal and transfected cells were collected and washed. Fluorescent labeling dyes, Annexin V and PI (Beyotime), were employed for apoptosis labeling and incubated for 30 minutes. Individual cells were analyzed for distinct fluorescence intensities using a flow cytometer (BD Biosciences). Data were processed with FlowJo software to obtain the percentage of apoptotic cells.

Cells were trypsinized, resuspended in a complete growth medium, and washed with PBS. Following overnight fixation in 70% cold ethanol, cells were stained using the Cell Cycle and Apoptosis Analysis Kit (Beyotime). Cell cycle distribution was determined using a flow cytometer (BD Biosciences), and data were analyzed and processed using FlowJo.

## 2.9 In vivo proliferation experiment

All animal procedures were approved by the Animal Ethics Committee of Tianjin Medical University. Four-week-old female BALB/c-nude mice were purchased from SPF (Beijing) Biotechnology Co., Ltd.  $1 \times 10^7$  MHCC97H cells with stable *ESCO2* knockdown or control RNA were subcutaneously injected into the right flank of each nude mouse ( $n = 5$  per group). On day 21, mice were euthanized, and tumors were excised. Tumor tissues were fixed, paraffin-embedded, sectioned, and stained with anti-Ki67 antibody (dilution 1:200, Affinity BioSciences, Cincinnati, OH, USA). Slide images were examined and quantified by a pathologist.

## 2.10 Statistical analysis

Analyses between the two groups were performed using the Wilcoxon test, while the one-way analysis of variance (ANOVA) test was utilized for comparisons involving three or more groups. All statistical calculations were performed using R Studio and GraphPad software.

## 3. Results

### 3.1 *ESCO2* is overexpressed in HCC tissues and associated with poor prognosis

Previous studies have demonstrated that *ESCO2* is markedly upregulated in lung, kidney, and colorectal malignancies [11-13]; however, no studies have focused on *ESCO2* expression in HCC. Using TCGA data, it was first identified that HCC samples exhibited significantly higher *ESCO2* mRNA levels than normal tissues (Figure 1A). *ESCO2* was significantly overexpressed in most HCC tissues using RNA-seq data from 50 matched cohorts of HCC and paracancerous tissues (Figure 1B). HCCDB database analysis of eight independent HCC study cohorts indicated that *ESCO2* expression was significantly higher in HCC tissues than normal ones (Figure 1C). Meanwhile, spatial transcriptomic data from two HCC leading-edge sections was employed to further confirm the overexpression of *ESCO2* in HCC tissues (Figure 1D). Finally, the protein level of *ESCO2* in HCC samples was significantly higher than in paracancerous samples (Figure 1E). These findings demonstrated that HCC tissues exhibited significant overexpression of *ESCO2* compared to nearby non-tumor tissues.

The potential of *ESCO2* as a prognostic biomarker was then explored, given its overexpression in HCC tissues. Kaplan-Meier survival analyses for HCC patients were performed using TCGA data to determine the relationship between *ESCO2* expression and prognosis, focusing on overall survival (OS), disease-free interval (DFI), disease-specific survival (DSS), and progression-free interval (PFI). Upregulated *ESCO2* expression was significantly associated with poor outcomes (Figure 2A). Next, the association between survival outcomes and *ESCO2* expression was evaluated in the ICGC cohort. Similarly, HCC patients with increased *ESCO2* expression demonstrated poor OS (Figure 2A). To further substantiate the involvement of *ESCO2* in cancer progression, the association between *ESCO2* expression and clinical data was evaluated. *ESCO2* expression value positively correlated with tumor stage, size, grade, and survival status (Figure 2B). The most common clinical indicators for assessing the progression of cancer are tumor stage, size, and grade.



Our analysis confirmed the positive correlation between ESCO2 and theses clinical indicators, implying that ESCO2 contributes to HCC progression. Furthermore, univariate and multivariate Cox regression analyses revealed that ESCO2 expression

was an independent prognostic indicator independent of other clinical factors (Figure 2C and 2D). Overall, our findings suggest ESCO2 as a potential promoter of HCC initiation and progression.

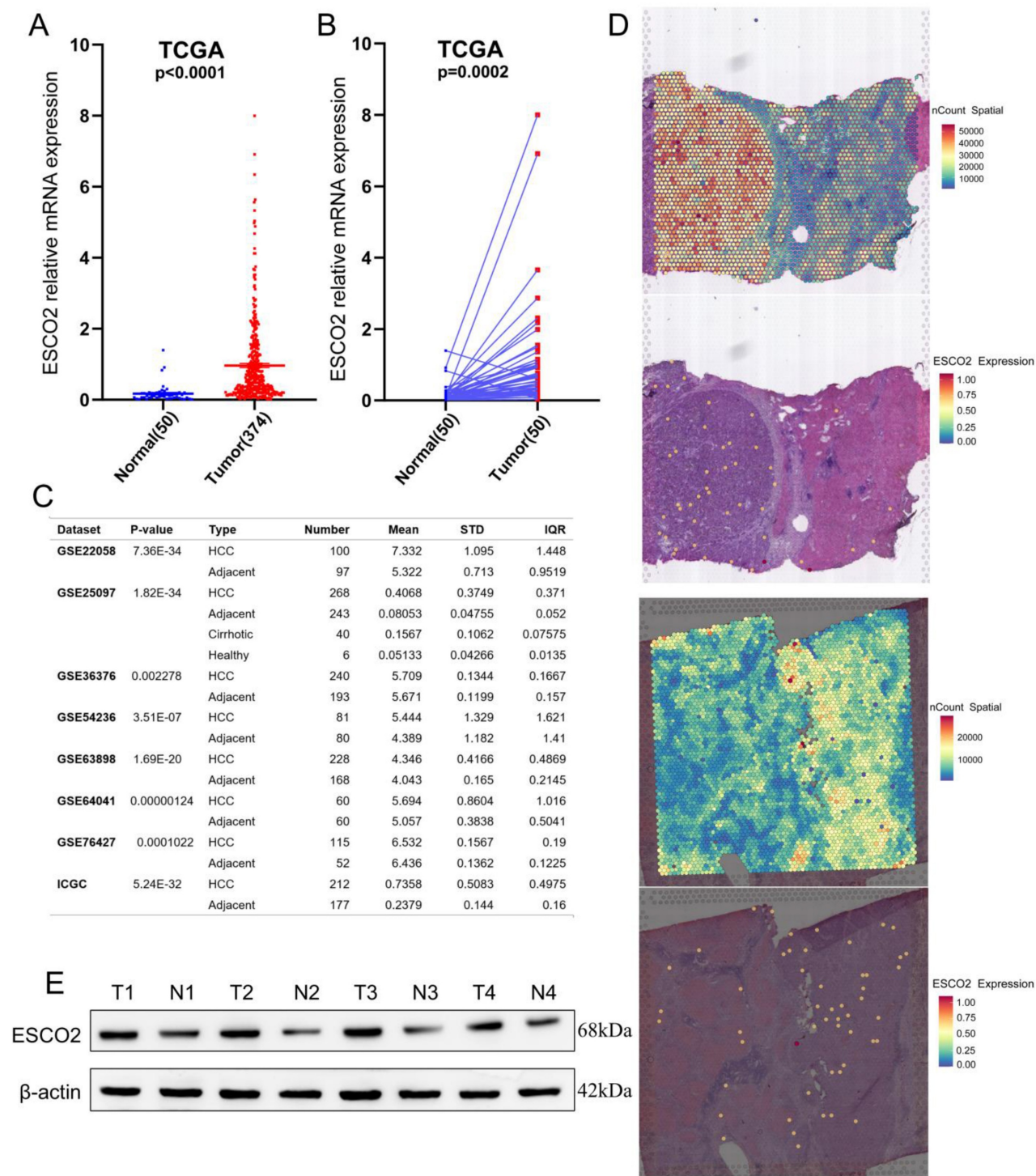


**Figure 1. ESCO2 is overexpressed in liver cancer tissues.** (A) Comparison of ESCO2 expression level between HCC and normal samples in TCGA database. (B) Comparison of ESCO2 expression levels between 50 paired HCC tissues and corresponding normal tissues. (C) Multiple HCC sequencing data from the HHCDB database was utilized to determine the expression levels of ESCO2 in HCC and normal tissues. (D) Spatial plots show the spatial expression pattern of ESCO2 in this study. (E) Western blot protein detection of the ESCO2 expression levels in adjacent normal tissues and paired HCC tissues. The optical density ratio of bands represent objective proteins to band of β-actin was calculated.

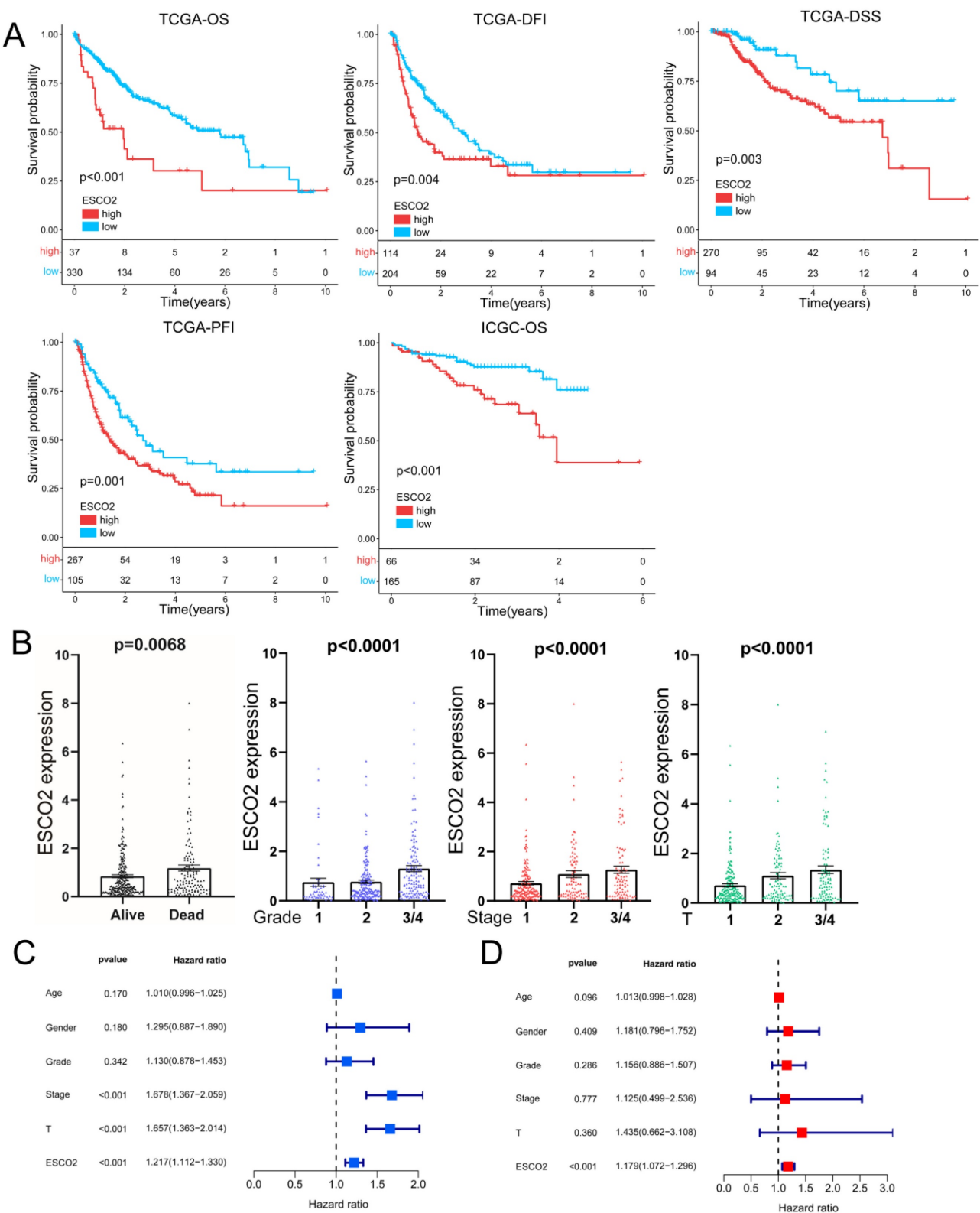


**Figure 2. ESCO2's Prognostic Value in HCC.** (A) The Kaplan–Meier survival curves stratified by ESCO2 expression level. The indicators include OS, DFI, DSS, and PFI. (B) Association between ESCO2 expression and tumor stage, tumor metastasis, tumor grade and survival state. (C) Univariate and multivariate(D) analyses showed that ESCO2 expression was a prognostic indicator independent of other clinical characteristics.

3.2 ESCO2 regulates the cell cycle

Our study demonstrated that ESCO2 is a reliable biomarker for HCC and further investigated the

effector function of ESCO2 in tumorigenesis. To explore the oncogenic role of this protein, HCC patients were divided into ESCO2-high and ESCO2-low subsets based on the median ESCO2

expression value. Gene Set Enrichment Analysis (GSEA) was performed to identify gene sets enriched in both groups. The top 10 most significant enriched pathways were visualized in this study. For the ESCO2-high subset, upregulated genes demonstrated enrichment in the G2M checkpoint, PI3K-AKT-MTOR signaling, and mTORC1 signaling pathways, which are associated with cell proliferation and cell cycle progression. Additionally, the apoptosis and p53 pathway was also significantly enriched in the ESCO2-high subset (Figure 3A). To further investigate the regulatory pathways of ESCO2, TCGA and ICGC data were utilized to identify ESCO2-related regulatory genes, as described in the methods section.

A total of 128 ESCO2-related regulatory genes were identified (Figure 3B). These genes showed enrichment in the cell cycle, mitotic cell cycle process, cell cycle phase transition, and mitotic cytokinesis (Figure 3C). To identify core genes, a protein-protein interaction (PPI) network of ESCO2-related regulatory genes was constructed using the STRING database [18]. The top 5 core genes were *CDK1*, *BUB1*, *BUB1B*, *CCNB1*, and *CCNB2*, all of which encode essential proteins for regulating the cell cycle (Figure 3D). Cyclin-dependent kinase 1 (CDK1) is essential for facilitating the G2/M transition, controlling the G1 process, and governing the G1-S transition [19].

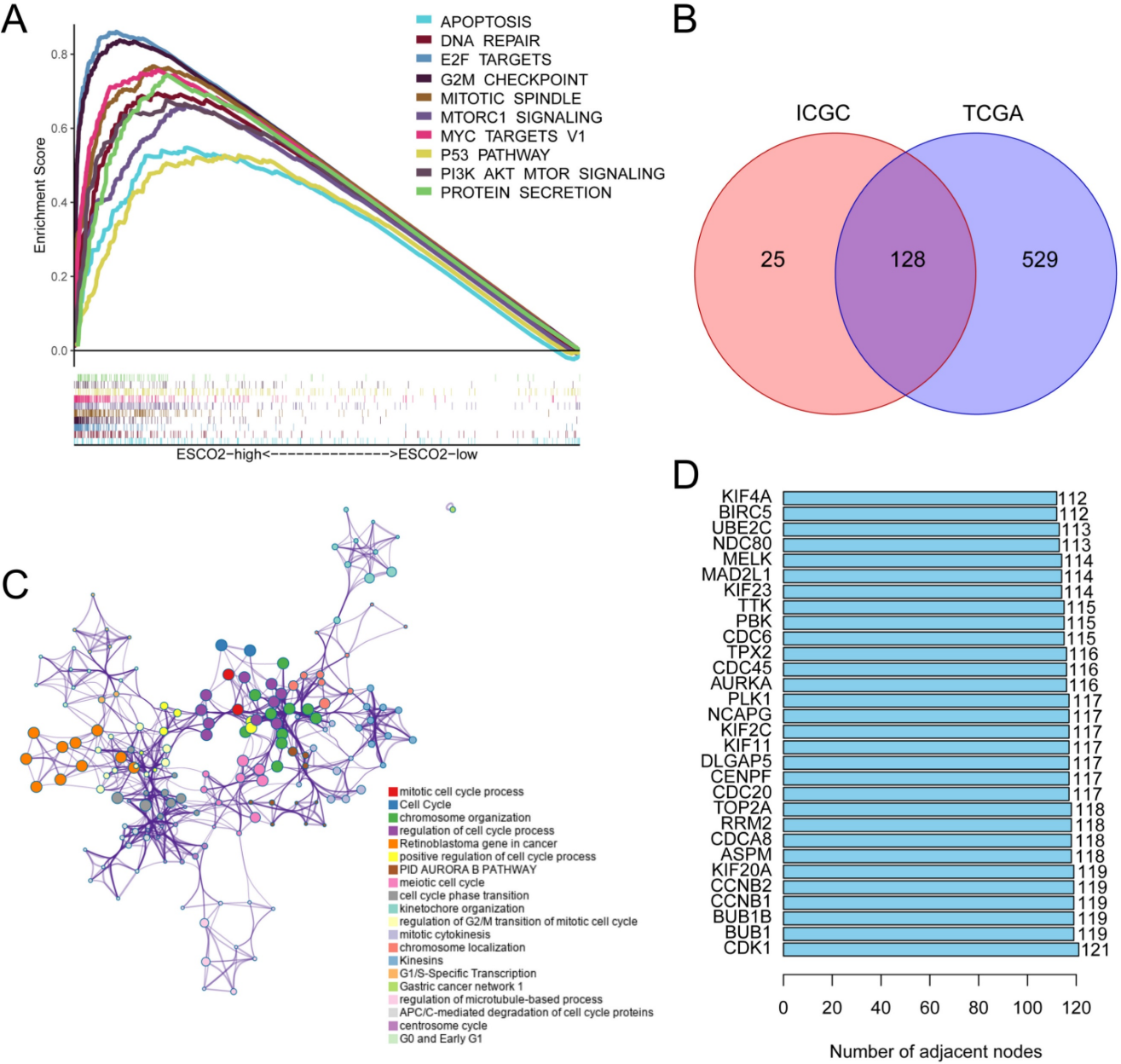


**Figure 3. ESCO2 regulates the cell cycle.** (A) The GSEA analysis between ESCO2-high and ESCO2-low groups in HCC. Each panel's left and right sides represent the enriched pathways of the ESCO2 high and low expression group, respectively. (B) The intersecting genes of DEGs between the ESCO2-high and ESCO2-low groups. (C) The ESCO2-related regulatory gene functions were mainly enriched in mitotic cell cycle and cell cycle. The interactive network was constructed using the Metascape online platform. (D) Bar plot of the top 30 genes with the largest number of adjacent nodes in the PPI network of ESCO2-related regulatory genes.



Numerous studies have demonstrated that CDK1 dysregulation leads to chromosomal instability, aggressive tumor growth, and accelerated cell proliferation [20]. CDK1 inhibitors are potential effective anti-cancer small-molecule drugs. For instance, in an HCC patient-derived xenograft (PDX) tumor model, treatment with the CDK1 inhibitor RO3306 in combination with sorafenib significantly decreased tumor growth [21]. Similarly, BUB1 and BUB1B are crucial for maintaining accurate chromosome segregation and reducing aneuploidy formation during mitosis [22]. Experiments have shown that BUB1 and BUB1B can promote cancer cell proliferation and are promising therapeutic targets [23-25]. The appropriate regulation of the G2/M transition phase depends on the presence of CCNB1 (Cyclin B1), located on chromosome 5q13.2. CCNB1 is aberrantly expressed in several malignancies and is highly associated with patient prognosis [26, 27]. HCC tissues exhibit significantly higher levels of CCNB1, and HCC cell proliferation can be suppressed by CCNB1 knockdown [28]. In conclusion, our bioinformatics analysis suggests that ESCO2 regulates pathways associated with the cell cycle.

### 3.3 Single-cell analysis of ESCO2

The tumor microenvironment (TME) is critical for tumor development and immune escape of tumor cells [29]. Stromal and immune cells within the TME are genetically stable, unlike tumor cells. Modifying TME components holds promise for overcoming the pervasive issue of immunotherapy resistance. As a result, current cancer research has shifted from a cancer cell-centric to a non-tumor cell-centric approach [30]. Due to the high heterogeneity and plasticity of the TME, oncogenes may play distinct roles in each cell type. Traditional bulk RNA sequencing data may not be sufficient to accurately assess the functional roles of oncogenes. To address this limitation, we employed single-cell analysis to explore the effector function of ESCO2 in malignant cells at the single-cell resolution. We found that myeloid cells, B cells, T/NK cells, and malignant cells expressed ESCO2 (Figure 4A and 4B). Hepatoma cells were then extracted and divided into ESCO2-positive and ESCO2-negative subgroups based on ESCO2 expression levels. GSVA results showed that E2F targets, G2M checkpoint, and MYC targets signaling pathways were enriched in ESCO2-positive cells, which aligns with our previous bioinformatics results (Figure 4C). Differential expression analysis was performed between ESCO2-positive and ESCO2-negative subgroups (Figure 4D). GO analysis revealed that the DEGs were primarily enriched in terms associated with proliferation, including

regulation of the mitotic cell cycle, nuclear division, and sister chromatid segregation. Furthermore, DEGs showed enrichment in DNA replication and cell cycle pathways in KEGG analysis (Figure 4E). Subsequently, when the cell cycle profiles of the two groups were compared, a higher proportion of ESCO2-positive group cells were observed in the G2/M phase, suggesting a more robust capacity for proliferation (Figure 4F).

### 3.4 ESCO2 knockdown inhibits the growth of HCC cells *in vitro* and *in vivo*

We first validated the knockdown efficiency of ESCO2-siRNA in hepatoma cell lines. Western blotting and PCR results confirmed that two siRNAs were effective in downregulating ESCO2 at both the mRNA and protein levels (Figure 5A and 5B). After confirming ESCO2's knockdown efficiency, several *in vitro* experiments were conducted to examine the impact of ESCO2 knockdown on the biological behavior of HCC cells. First, the CCK-8 assay revealed that in Huh7 cell lines, the absorbance of the siRNA1# and siRNA2# groups was significantly lower than the si-NC group at 24 h, 48 h, and 72 h (Figure 5C). Similarly, the colony formation assay demonstrated that at day 11, a significantly smaller number of cell colonies were formed following ESCO2 knockdown (Figure 5D). Intriguingly, the EdU assay revealed that the proliferation of HCC cells was significantly inhibited by ESCO2 knockdown (Figure 5E). Similarly, the knockdown of ESCO2 in MHCC97H cells significantly inhibited its proliferative ability (Figure 6A-E). The results presented above collectively indicated that ESCO2 knockdown suppressed the proliferative capacity of hepatoma cell lines.

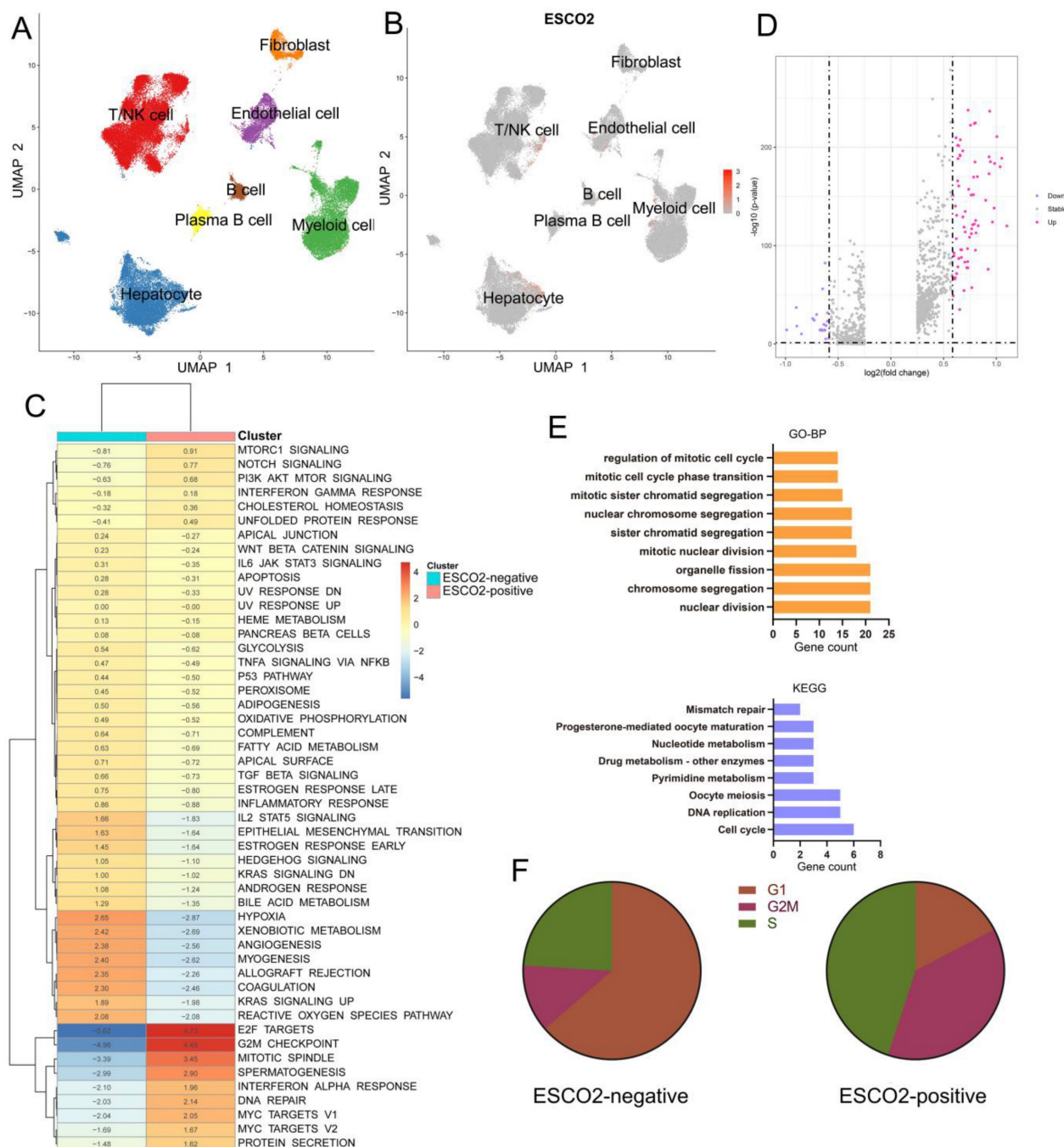
Due to the higher knockdown efficiency of siRNA-1, we then constructed a lentivirus using the sequence of siRNA-1 for subsequent experiments. We then constructed a subcutaneous xenograft mouse model to examine the effects of regulating ESCO2 expression on HCC cell proliferation *in vivo*. MHCC97H cells stably transfected with sh-ESCO2 or sh-Control were injected into the flanks of nude mice, and tumor volumes were recorded periodically. Tumor volume and weight were significantly reduced in the sh-ESCO2 group compared to the sh-Control group (Figure 7A and 7B). Tumors were then excised for immunohistochemical (IHC) analysis. The results showed that the Ki-67 level was substantially lower in mice injected with ESCO2-knockdown MHCC97H cells compared to the corresponding control mice (Figure 7C and 7D). Taken together, these findings demonstrate that ESCO2 could promote the growth of HCC cells both *in vivo* and *in vitro*.



### 3.5 Knockdown of ESCO2 inhibits HCC cell proliferation by inducing G1-S cell cycle arrest and stimulating apoptosis *in vitro*

According to our bioinformatics investigation, ESCO2 primarily participates in cell cycle regulation. Therefore, flow cytometry was performed to analyze the cell cycle distribution of HCC cells after *ESCO2* knockdown. Compared to the sh-NC group, the sh-ESCO2 group exhibited a significantly larger

percentage of cells in the G1 phase (Figure 8A). This finding indicated that *ESCO2* knockdown could induce S-phase arrest in HCC cells. Additionally, apoptosis-related flow cytometry results revealed that the proportion of apoptotic cells in both the MHCC97H and Huh7 cell lines was significantly higher in the sh-ESCO2 group compared to the sh-NC group (Figure 8B). Consequently, *ESCO2* knockdown could induce apoptosis in HCC cells.



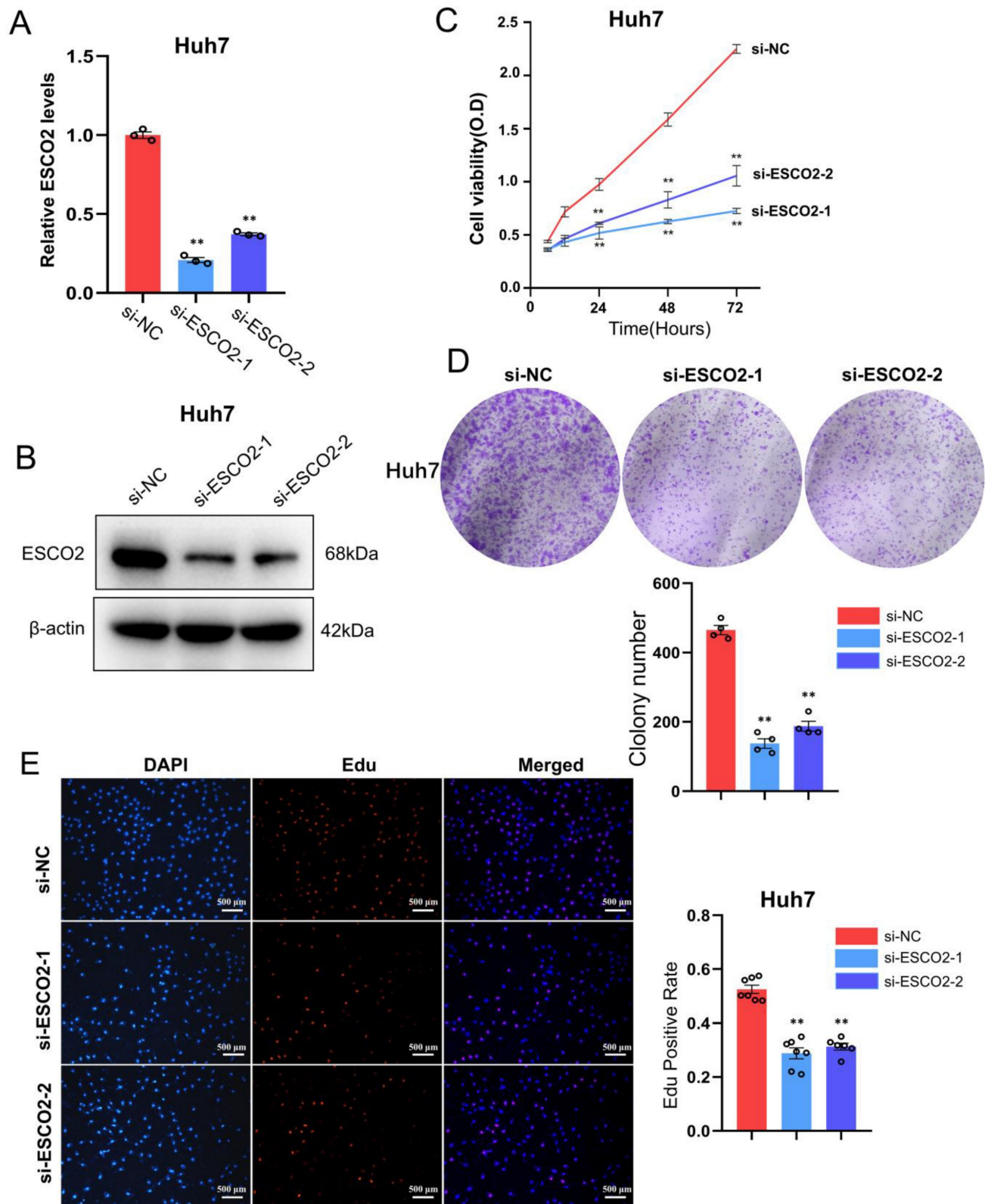
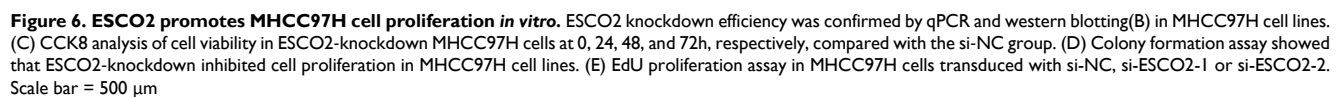


**Figure 5. ESCO2 promotes Huh7 cell proliferation *in vitro*.** ESCO2 knockdown efficiency was confirmed by qPCR and western blotting (B) in Huh7 cell lines. (C) CCK8 analysis of cell viability in ESCO2-knockdown HCC cells at 0, 24, 48, and 72h, respectively, compared with the si-NC group. (D) Colony formation assay showed that ESCO2-knockdown inhibited cell proliferation in Huh7 cell lines. (E) EdU proliferation assay in Huh7 cells transduced with si-NC, si-ESCO2-1 or si-ESCO2-2. Scale bar = 500  $\mu$ m.



ESCO2 knockdown prevents HCC cell growth by inducing G1-S phase cell cycle arrest and apoptosis. First, in Huh7 and MHCC97H cell lines, Western blotting of cell cycle-related proteins revealed that the sh-NC group exhibited increased levels of CDK1 and cyclin B1 expression compared to the sh-ESCO2



group. Additionally, CDK2 and cyclin A2 protein expression was significantly decreased after *ESCO2* knockdown (Figure 9A). These findings suggest that *ESCO2* knockdown induces cell cycle arrest by regulating the CDK1/CDK2 signaling pathways. Subsequently, Western blotting of apoptosis-related proteins demonstrated that inhibition of *ESCO2* significantly increased the expression levels of pro-apoptotic proteins (BAX and Caspase-3). Conversely, compared to the sh-NC group, the sh-*ESCO2* group displayed significantly decreased expression of the anti-apoptotic protein BCL-2 (Figure 9B). Hence, *ESCO2* knockdown can trigger apoptosis in HCC cells by regulating these apoptosis-specific proteins. Meanwhile, considering the GSEA results suggesting that *ESCO2* might be involved in the

regulation of the PI3K/AKT/mTOR signaling pathway, and given the frequent activation of the PI3K/AKT/mTOR pathway in cancer and its crucial role in regulating cell cycle and apoptosis, we investigated how *ESCO2* knockdown affected the PI3K/AKT/mTOR pathway. The band intensities of phosphorylated PI3K, AKT, and mTOR were significantly weaker in sh-*ESCO2* cells compared to control cells, indicating that knockdown of *ESCO2* significantly inhibited the PI3K/AKT/mTOR pathway (Figure 9C). In summary, *ESCO2* may influence the expression of proteins involved in the cell cycle and apoptosis by activating the PI3K/AKT/mTOR signaling pathway, which supports the growth of HCC cells.

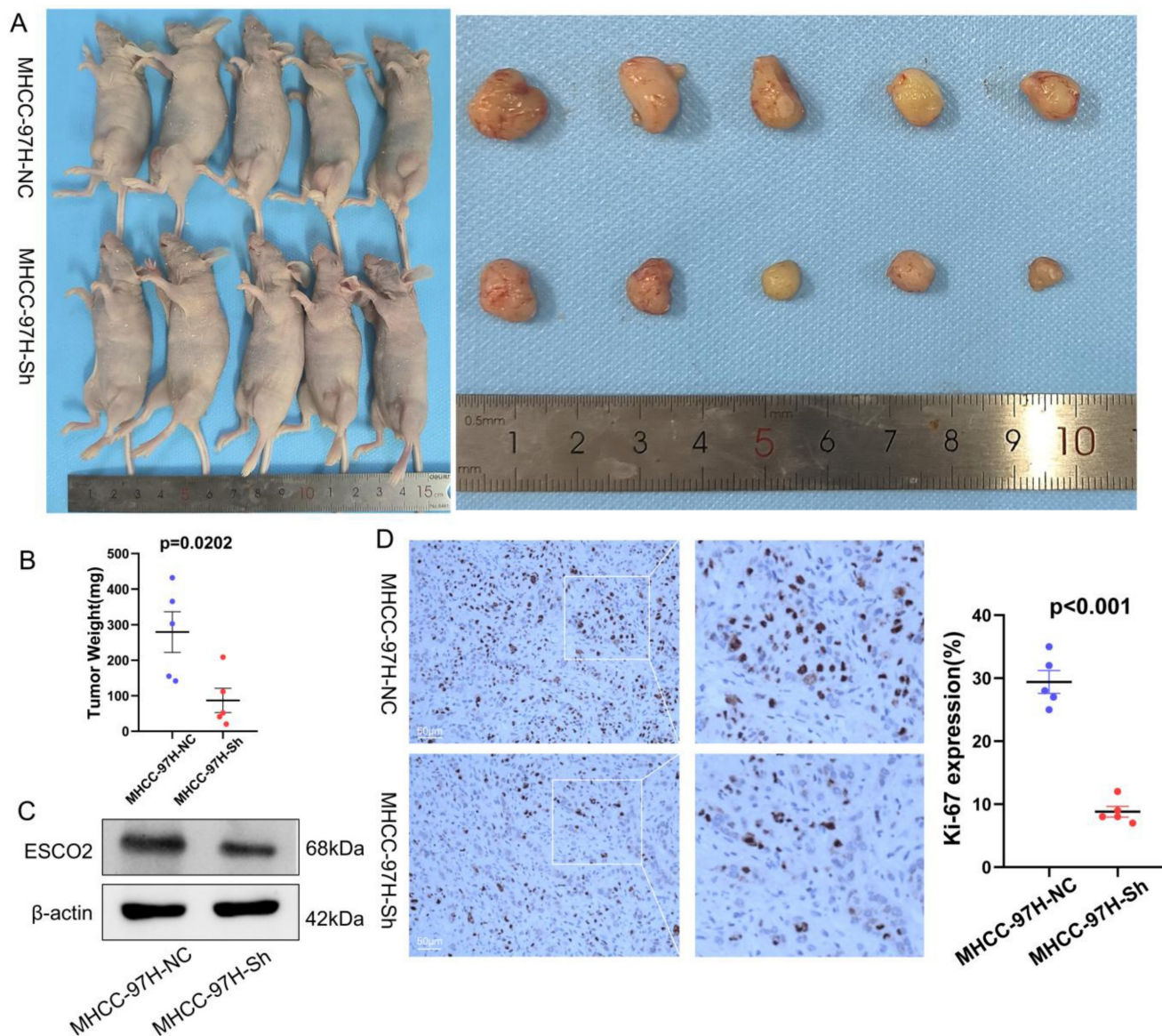


**Figure 7. *ESCO2* promotes MHCC97H cell proliferation in vivo.** (A) The images of the subcutaneous tumors formed in nude mice between the scramble and *ESCO2*-knockdown groups. (B) Comparing the tumor weight of the *ESCO2*-knockdown and scrambling groups statistically. (C) *ESCO2* was efficiently knocked down in tumor tissue formed in nude mice, as determined by western blotting. (D) IHC analysis of the xenograft tumor tissues' Ki-67 expression levels in the *ESCO2*-knockdown and scramble groups.



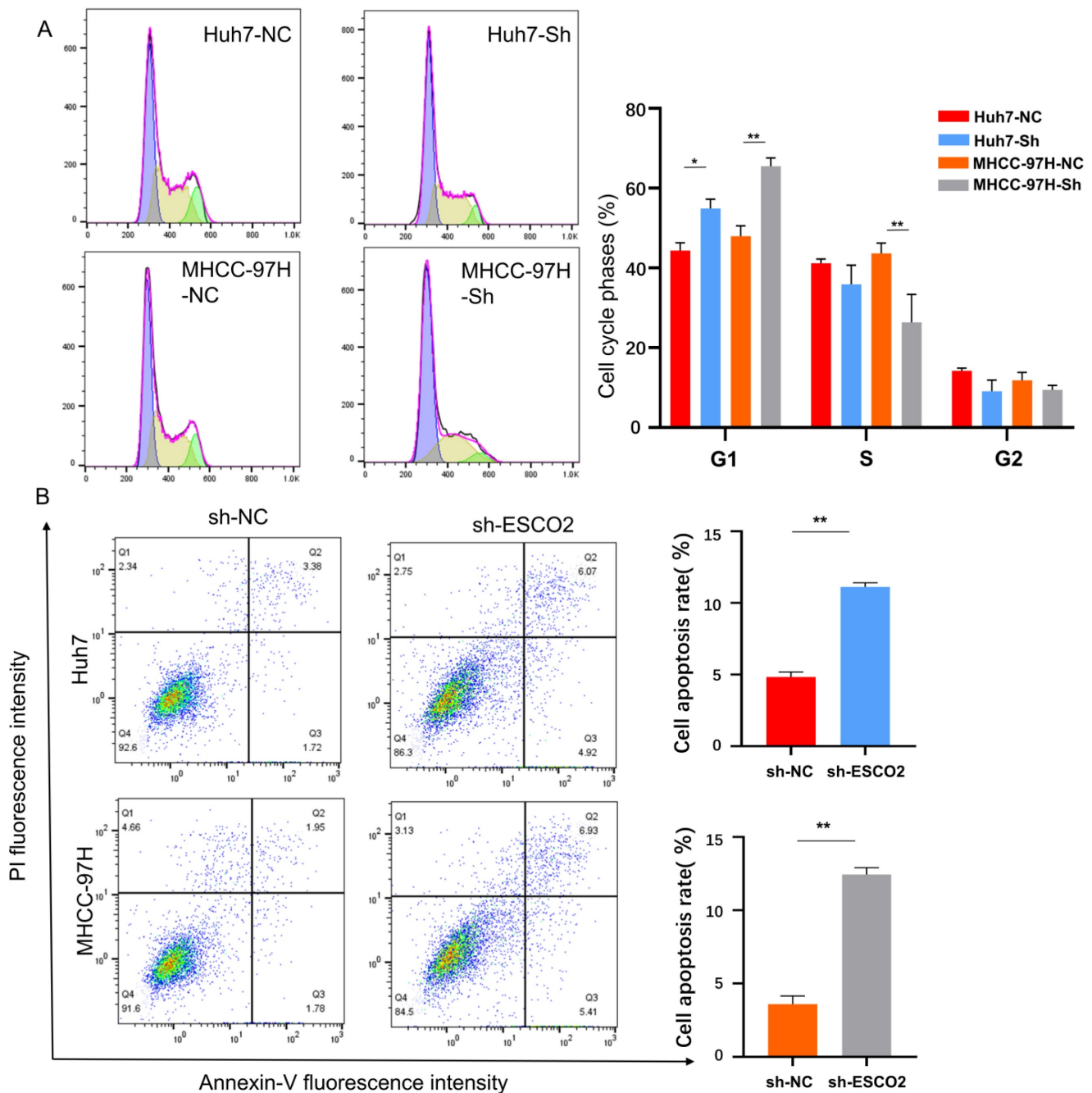


**Figure 8.** (A) Results and statistics of cell cycle-related flow cytometry for HCC cells in the sh-NC group and sh-ESCO2 group. (B) Flow cytometry results and statistics related to apoptosis of HCC cells.

## Discussion

Advanced HCC is characterized by a poor prognosis. Despite significant advancements in systemic therapy that have increased survival time in this population, the median overall survival remains extremely short. As the current first-line treatment for advanced HCC, atezolizumab/bevacizumab therapy has demonstrated superior efficacy and tolerability compared to sorafenib [31]. Other drug combination treatment options are currently being tested. Therefore, the effective combination of

immunotherapy and targeted medicine is a research highlight to further improve the prognosis of advanced HCC patients. Advancements in sequencing technology present greater possibilities for identifying diagnostic and therapeutic targets that could benefit HCC patients through early detection, precise treatment, and prognostic monitoring. Cell division and cell death are fundamental processes that govern organism growth and development. Both processes are abnormally regulated in cancer, leading to uncontrolled proliferation [32]. Uncontrolled cancer growth and metastasis are the primary causes

of liver cancer's high mortality and recurrence rates. Understanding the mechanisms underlying HCC proliferation would aid in discovering innovative and more effective therapeutic strategies to improve survival rates. In previous studies, *ESCO2* was identified as a potential target for cancer therapy, as it is a pivotal protein in the cell division process. Acetylation of the SMC3 subunit of the cohesin protein by *ESCO2* acetyltransferase facilitates SCC. The cohesion of the cohesin protein complex between sister chromatids ensures accurate chromosomal segregation [33, 34]. *ESCO2* was significantly elevated

in tumor tissues in several malignancies, and *ESCO2* knockdown could inhibit cancer cell proliferation, invasion, and migration. However, the underlying mechanism of *ESCO2* upregulation in cancer development remains incompletely understood. The potential of *ESCO2* as a therapeutic target for HCC is unknown. Our research elucidates the mechanism by which *ESCO2* promotes HCC proliferation. Accordingly, *ESCO2* may serve as a valuable molecular diagnostic marker and potential therapeutic target for HCC patients.

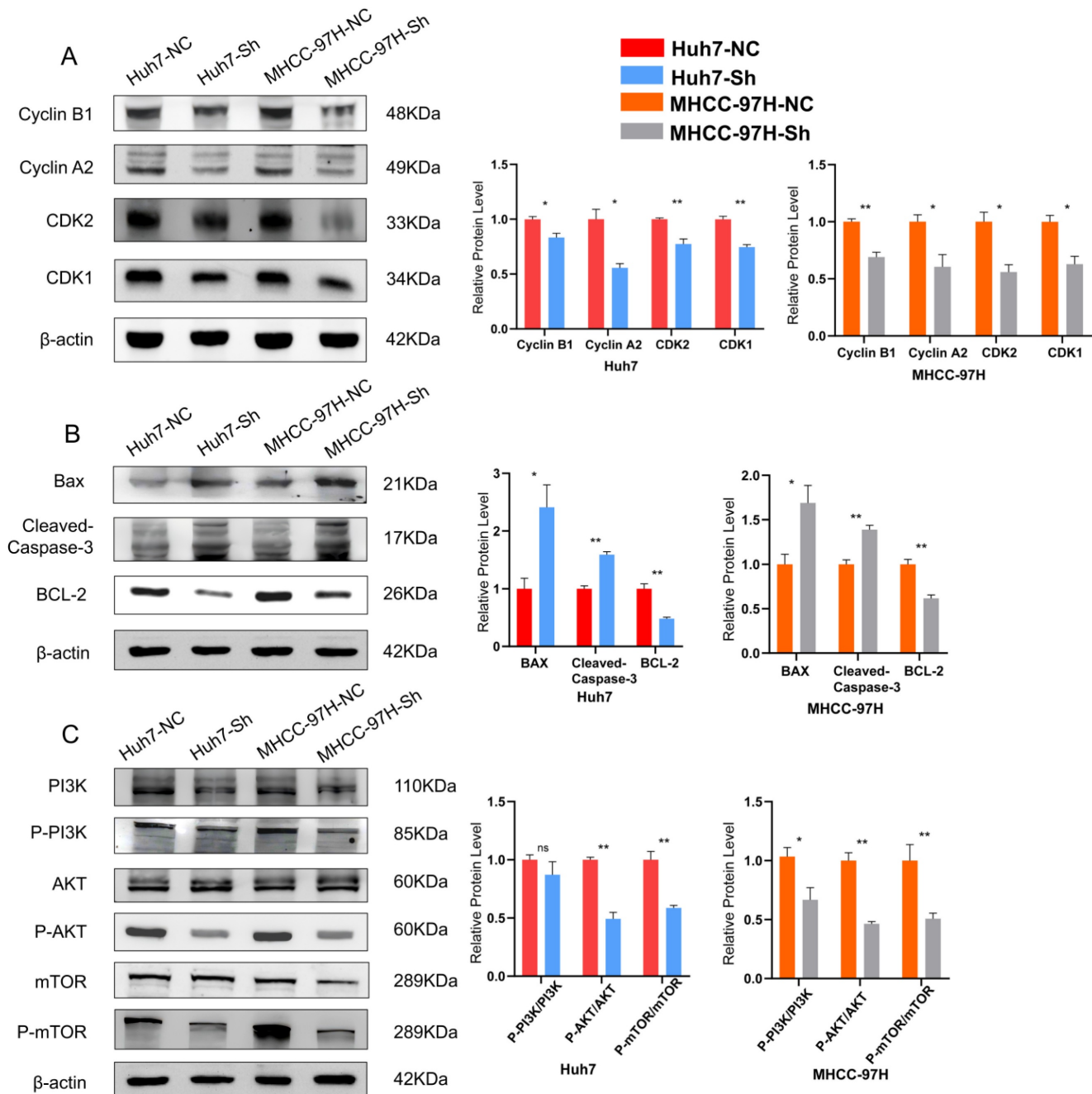


**Figure 9. *ESCO2* regulates HCC proliferation via the PI3K/AKT/mTOR signaling pathway.** (A) Western blot results and statistics of cell cycle-related proteins of HCC cells. (B) Western blot results and statistics of cell apoptosis-related proteins of HCC cells. (C) Western blot analysis showing the levels of P-PI3K, P-AKT and P-mTOR when *ESCO2* was knocked down.

Our study provided hitherto undocumented evidence that *ESCO2* expression was significantly upregulated in HCC tissues using extensive HCC sequencing data. Leveraging public databases, our data included 1446 HCC tissues and 943 normal tissues, enhancing the robustness of our findings. More importantly, we identified that HCC samples possessed a significantly higher *ESCO2* protein level than paracancerous samples. Given the high expression of *ESCO2* in HCC tissues, it may function as an oncogene that promotes hepatocarcinogenesis. Furthermore, upregulated *ESCO2* expression was strongly associated with worse outcomes in HCC patients. *ESCO2* expression positively correlated with tumor grade, size, and stage. To some extent, tumor stage and grade represent the progression of liver cancer. Hence, *ESCO2* may significantly contribute to HCC progression. Finally, we verified that *ESCO2* was an independent prognostic indicator for HCC patients. Based on the aforementioned findings, *ESCO2* is a reliable biomarker for HCC patients. Oncogenes are known to impact the biological behavior of cancer cells (migration, invasion, and proliferation), thereby facilitating cancer progression. Bioinformatic analysis suggested that *ESCO2* expression was closely related to hepatocarcinogenesis and development. Therefore, we employed siRNA to inhibit *ESCO2* expression in HCC cell lines. Our cellular experiments supported the conclusion that *ESCO2* knockdown significantly suppressed the proliferative ability of HCC cell lines. Additionally, the subcutaneous xenograft nude mouse model confirmed that *ESCO2* could promote the growth of HCC cells *in vivo*. Consequently, we confirmed that *ESCO2*, a potential oncogene, may promote HCC growth and lead to a poor prognosis by inducing the malignant biological behavior of HCC cells. Previous studies have shown that *ESCO2* could enhance the proliferative and migratory capacities of lung, kidney, and stomach cancer cells. Our findings aligned with these previous reports.

Oncogenes typically regulate cancer cell biology by modifying cellular signaling pathways. Previous research found that *ESCO2* affects the AKT/mTOR pathway in kidney cancer [11]. *ESCO2* knockdown inhibited mTOR/RPS6K1 activation and upregulated AMPK $\alpha$  and p53 phosphorylation in gastric cancer cells [35]. In lung cancer, *ESCO2* acetylates hnRNPA1, maintaining it in the nucleus and ultimately enhancing aerobic glycolysis by increasing PKM2 and decreasing PKM1 expression [12]. In the present study, we first explored the effector function of *ESCO2* in HCC using bioinformatic methods. GSEA results revealed that *ESCO2* participates in E2F targets, G2M checkpoint, PI3K-AKT-MTOR signaling,

and mTORC1 signaling pathways, which are associated with cell cycle and proliferation. We also identified 128 *ESCO2*-related regulatory genes. These genes showed enrichment in the cell cycle, mitotic cell cycle process, cell cycle phase transition, and mitotic cytokinesis. Moreover, our study explored the biological function of *ESCO2* at the single-cell level, which avoids the interference of other non-tumor cells. Consistent with the results of bulk RNA sequencing data analysis, cell proliferation-associated pathways, such as E2F targets, G2M checkpoint, and MYC targets signaling, were significantly enriched in *ESCO2*-positive hepatoma cells. Overall, our bioinformatic analysis suggests that *ESCO2* plays a significant role in regulating cell cycle and cell proliferation-related pathways.

We next explored *ESCO2*'s role in regulating the cell cycle and cell growth through a series of experiments. Flow cytometry demonstrated a significantly larger percentage of HCC cells in the G1 phase after *ESCO2* knockdown. Besides, *ESCO2* knockdown regulated the expression levels of HCC cell cycle proteins (CDK1, cyclin B1, CDK2, and cyclin A2), resulting in cell cycle arrest at the G1 phase. Cyclin B1 is a crucial cyclin that regulates the G2/M phase. During the S and G2 phases of the cell cycle, cyclin B is synthesized in significant amounts, enters the nucleus, binds to CDK1, and activates the G2 to M phase transition [26]. Similarly, cyclin A2 (CCNA2) is a regulator of essential CDK protein kinases. Cyclin A2 binds and activates CDK2, thereby promoting the transition through the G1/S and G2/M phases [36]. Hence, *ESCO2* knockdown induces cell cycle arrest by regulating the CDK1/CDK2 signaling pathway. Human malignancies frequently exhibit cell cycle dysregulation, and targeting cell cycle proteins is one of the most promising areas for cancer therapy. Scientists have demonstrated the effectiveness of targeting proteins associated with the cell cycle to limit tumor growth. For instance, researchers identified that homoharringtonine (HHT) could bind to the PPI site of CDK2, disrupting the interaction between CDK2 and cyclin A, resulting in a loss of CDK2 activity and protein degradation, and preventing tumor progression [37]. Additionally, all three CDK4/6 inhibitors have been approved by the United States Food and Drug Administration (FDA) for breast cancer treatment [38]. Therefore, *ESCO2* may be a promising target for cell cycle-related protein targeting. Furthermore, we discovered that *ESCO2* knockdown induced apoptosis in HCC cells. Western blotting results showed that knockdown of *ESCO2* increased the levels of apoptosis-related proteins (BAX, Caspase-3), promoting apoptosis in HCC cells. Apoptosis is a crucial step in the death of

tumor cells. Evasion of apoptosis contributes to cancer cell escape and treatment resistance. Consequently, many cancer therapies rely on successful apoptotic induction [39]. Numerous drugs targeting apoptosis-related proteins have been developed with promising outcomes [40]. Furthermore, our research revealed that ESCO2 regulates cell cycle and apoptosis by activating the PI3K/AKT/mTOR pathway. The PI3K/Akt/mTOR signaling pathway is indispensable in many cellular biological processes, including cell proliferation, survival, metabolism, motility, angiogenesis, and response to stress and therapy. Extensive research supports its critical role in regulating tumor growth, metabolism, metastasis, and treatment resistance [41, 42]. Small-molecule inhibitors targeting key kinases in the PI3K/Akt/mTOR pathway have been developed and evaluated in preclinical models and human clinical trials. For instance, the FDA approved idelalisib, a PI3K inhibitor, to treat follicular B-cell non-Hodgkin's lymphoma and relapsed chronic lymphocytic leukemia [43]. Currently, there are over 35 clinical trials targeting the PI3K/Akt/mTOR pathway in HCC. However, outcomes indicated that the clinical benefit of monotherapy with these inhibitors remains limited [44]. This may be due to the interaction of the PI3K/Akt/mTOR pathway with multiple signaling pathways, increasing the likelihood of adverse events and treatment resistance. Combination therapy may be a more effective strategy for advanced HCC. Understanding the crosstalk and feedback with other pathways will, therefore, be key challenges in targeting the PI3K/Akt/mTOR pathway. Future studies should explore the upstream and downstream regulatory mechanisms of the PI3K/Akt/mTOR pathway, which will provide crucial insights for developing novel therapeutic targets or proposing innovative combination therapeutic regimens. Our study will provide valuable insights for the development of drugs targeting the PI3K/Akt/mTOR pathway.

Herein, we determined that ESCO2 was significantly upregulated in HCC tissues and linked to a poorer prognosis. Knockdown of ESCO2 significantly inhibited HCC cell proliferation both *in vivo* and *in vitro*. Most notably, ESCO2 could promote the PI3K/AKT/mTOR pathway, accelerating the cell cycle and inhibiting apoptosis, and thus increasing HCC growth. These findings offer innovative and valuable insights for targeted therapy in HCC.

However, this study has some limitations that should be acknowledged. First, investigations into the specific mechanism of ESCO2's involvement in HCC remain insufficient, which is a focus for future studies. Additionally, our study lacks a real-world clinical

cohort to assess the predictive power of ESCO2 for prognosis in HCC.

## Conclusion

In summary, our study reveals for the first time the molecular mechanism by which ESCO2 promotes HCC proliferation. ESCO2 may activate the PI3K/AKT/mTOR pathway, thereby accelerating the cell cycle and inhibiting apoptosis, and consequently increasing HCC growth. Overall, this work identifies a novel HCC target gene, providing valuable insights for HCC prognostic assessment and molecular therapy.

## Supplementary Material

Supplementary table 1 and table 2 legend.  
<https://www.jcancer.org/v16p2929s1.pdf>

Supplementary table 2.  
<https://www.jcancer.org/v16p2929s2.xlsx>

## Acknowledgements

### Funding

This work was supported by the National Natural Science Foundation project (82372194), Tianjin Health Science and Technology Project (TJWJ2023MS012) and Nankai University Institute of Transplant Medicine Independent Project (NKTm2023003).

### Author contributions

The research scheme was developed by DPC and YH, who also carried out the bioinformatics analysis. YH, DPC and WXZ performed the experiments. YCZ and WXZ collected and organized the gene expression matrix. DPC and YH wrote the manuscript. YB and YMZ provided administrative assistance while critically examining the article for crucial intellectual content. YB and YMZ were the guarantors for this study.

### Ethics approval and consent to participate

The authors confirm that all methods were conducted according to the principles of the Declaration of Helsinki and were approved by The Institutional Review Committee and the Medical Ethics Committee of the Tianjin First central hospital. Written informed consents have been obtained from all subjects.

### Data availability

The datasets involved in our work are available in the TCGA (<https://portal.gdc.cancer.gov/>), ICGC (<https://dcc.icgc.org/>), GEO (GSE149614,



<https://www.ncbi.nlm.nih.gov/geo/>) and GSA (<https://ngdc.cncb.ac.cn/gsa/>).

## Competing Interests

The authors have declared that no competing interest exists.

## References

- Sung H, Ferlay J, Siegel RL, Laversanne M, Soerjomataram I, Jemal A, et al. Global Cancer Statistics 2020: GLOBOCAN Estimates of Incidence and Mortality Worldwide for 36 Cancers in 185 Countries. *CA Cancer J Clin.* 2021; 71: 209-49.
- Llovet J M, et al. Hepatocellular carcinoma. *Nat Rev Dis Primers.* 2021; 7: 6.
- Siegel RL, Miller KD, Wagle NS, Jemal A. Cancer statistics, 2023. *CA Cancer J Clin.* 2023; 73: 17-48.
- Yang C, Zhang H, Zhang L, Zhu AX, Bernards R, Qin W, et al. Evolving therapeutic landscape of advanced hepatocellular carcinoma. *Nat Rev Gastroenterol Hepatol.* 2023; 20: 203-22.
- Fan Y, Xue H, Zheng H. Systemic Therapy for Hepatocellular Carcinoma: Current Updates and Outlook. *J Hepatocell Carcinoma.* 2022; 9: 233-63.
- Sia D, Villanueva A, Friedman SL, Llovet JM. Liver Cancer Cell of Origin, Molecular Class, and Effects on Patient Prognosis. *Gastroenterology.* 2017; 152: 745-61.
- Zhang T, Wang B, Gu B, Su F, Xiang L, Liu L, et al. Genetic and Molecular Characterization Revealed the Prognosis Efficiency of Histone Acetylation in Pan-Digestive Cancers. *J Oncol.* 2022; 2022: 3938652.
- Bender D, Da Silva E, Chen J, Poss A, Gawey L, Rulon Z, et al. Multivalent interaction of ESCO2 with the replication machinery is required for sister chromatid cohesion in vertebrates. *Proc Natl Acad Sci U S A.* 2020; 117: 1081-9.
- Kawasumi R, Abe T, Psakhye I, Miyata K, Hirota K, Branzei D. Vertebrate CTF18 and DDX11 essential function in cohesion is bypassed by preventing WAPL-mediated cohesin release. *Genes Dev.* 2021; 35: 1368-82.
- Vega H, Waisfisz Q, Gordillo M, Sakai N, Yanagihara I, Yamada M, et al. Roberts syndrome is caused by mutations in ESCO2, a human homolog of yeast ECO1 that is essential for the establishment of sister chromatid cohesion. *Nat Genet.* 2005; 37: 468-70.
- Wang QL, Liu L. Establishment of cohesion 1 homolog 2 facilitates cell aggressive behaviors and induces poor prognosis in renal cell carcinoma. *J Clin Lab Anal.* 2020; 34: e23163.
- Zhu HE, Li T, Shi S, Chen DX, Chen W, Chen H. ESCO2 promotes lung adenocarcinoma progression by regulating hnRNPA1 acetylation. *J Exp Clin Cancer Res.* 2021; 40: 64.
- Guo XB, Huang B, Pan YH, Su SG, Li Y. ESCO2 inhibits tumor metastasis via transcriptionally repressing MMP2 in colorectal cancer. *Cancer Manag Res.* 2018; 10: 6157-66.
- Lu Y, Yang A, Quan C, Pan Y, Zhang H, Li Y, et al. A single-cell atlas of the multicellular ecosystem of primary and metastatic hepatocellular carcinoma. *Nat Commun.* 2022; 13: 4594.
- Wu R, Guo W, Qiu X, Wang S, Sui C, Lian Q, et al. Comprehensive analysis of spatial architecture in primary liver cancer. *Sci Adv.* 2021; 7: eabg3750.
- Elyada E, Bolisetty M, Laise P, Flynn WF, Courtois ET, Burkhart RA, et al. Cross-Species Single-Cell Analysis of Pancreatic Ductal Adenocarcinoma Reveals Antigen-Presenting Cancer-Associated Fibroblasts. *Cancer Discov.* 2019; 9: 1102-23.
- Yu G, Wang LG, Han Y, He QY. clusterProfiler: an R package for comparing biological themes among gene clusters. *OMICS.* 2012; 16: 284-7.
- Szklarczyk D, Kirsch R, Koutrouli M, Nastou K, Mehryary F, Hachilif R, et al. The STRING database in 2023: protein-protein association networks and functional enrichment analyses for any sequenced genome of interest. *Nucleic Acids Res.* 2023; 51: D638-638D646.
- Santamaria D, Barrière C, Cerqueira A, Hunt S, Tardy C, Newton K, et al. Cdk1 is sufficient to drive the mammalian cell cycle. *Nature.* 2007; 448: 811-5.
- Malumbres M, Barbacid M. Cell cycle, CDKs and cancer: a changing paradigm. *Nat Rev Cancer.* 2009; 9: 153-66.
- Wu CX, Wang XQ, Chok SH, Man K, Tsang S, Chan A, et al. Blocking CDK1/PDK1/ $\beta$ -Catenin signaling by CDK1 inhibitor RO3306 increased the efficacy of sorafenib treatment by targeting cancer stem cells in a preclinical model of hepatocellular carcinoma. *Theranostics.* 2018; 8: 3737-50.
- Elowe S, Bolanos-Garcia VM. The spindle checkpoint proteins BUB1 and BUBR1 (SLIM)ming down to the basics. *Trends Biochem Sci.* 2022; 47: 352-66.
- Zhou X, Yuan Y, Kuang H, Tang B, Zhang H, Zhang M. BUB1B (BUB1 Mitotic Checkpoint Serine/Threonine Kinase B) promotes lung adenocarcinoma by interacting with Zinc Finger Protein ZNF143 and regulating glycolysis. *Bioengineered.* 2022; 13: 2471-85.
- Song J, Ni C, Dong X, Sheng C, Qu Y, Zhu L. bub1 as a potential oncogene and a prognostic biomarker for neuroblastoma. *Front Oncol.* 2022; 12: 988415.
- Jiao CY, Feng QC, Li CX, Wang D, Han S, Zhang YD, et al. BUB1B promotes extrahepatic cholangiocarcinoma progression via JNK/c-Jun pathways. *Cell Death Dis.* 2021; 12: 63.
- Zhang H, Zhang X, Li X, Meng WB, Bai ZT, Rui SZ, et al. Effect of CCNB1 silencing on cell cycle, senescence, and apoptosis through the p53 signaling pathway in pancreatic cancer. *J Cell Physiol.* 2018; 234: 619-31.
- Chen X, Ma J, Wang X, Zi T, Qian D, Li C, et al. CCNB1 and AURKA are critical genes for prostate cancer progression and castration-resistant prostate cancer resistant to vinblastine. *Front Endocrinol (Lausanne).* 2022; 13: 1106175.
- Li M, Shang H, Wang T, Yang SQ, Li L. Huanglian decoction suppresses the growth of hepatocellular carcinoma cells by reducing CCNB1 expression. *World J Gastroenterol.* 2021; 27: 939-58.
- Xiao Y, Yu D. Tumor microenvironment as a therapeutic target in cancer. *Pharmacol Ther.* 2021; 221: 107753.
- Babar Q, Saeed A, Tabish TA, Sarwar M, Thorat ND. Targeting the tumor microenvironment: Potential strategy for cancer therapeutics. *Biochim Biophys Acta Mol Basis Dis.* 2023; 1869: 166746.
- Yan T, Yu L, Zhang N, Peng C, Su G, Jing Y, et al. The advanced development of molecular targeted therapy for hepatocellular carcinoma. *Cancer Biol Med.* 2022; 19: 802-17.
- Loftus LV, Amend SR, Pienta KJ. Interplay between Cell Death and Cell Proliferation Reveals New Strategies for Cancer Therapy. *Int J Mol Sci.* 2022; 23: 4723.
- Jevitt AM, Rankin BD, Chen J, Rankin S. The cohesin modifier ESCO2 is stable during DNA replication. *Chromosome Res.* 2023; 31: 6.
- Alomer RM, da Silva E, Chen J, Piekarz KM, McDonald K, Sansam CG, et al. Esco1 and Esco2 regulate distinct cohesin functions during cell cycle progression. *Proc Natl Acad Sci U S A.* 2017; 114: 9906-11.
- Chen H, Zhang L, He W, Liu T, Zhao Y, Chen H, et al. ESCO2 knockdown inhibits cell proliferation and induces apoptosis in human gastric cancer cells. *Biochem Biophys Res Commun.* 2018; 496: 475-81.
- Bendris N, Lemmers B, Blanchard JM, Arsic N. Cyclin A2 mutagenesis analysis: a new insight into CDK activation and cellular localization requirements. *PLoS One.* 2011; 6: e22879.
- Zhang J, Gan Y, Li H, Yin J, He X, Lin L, et al. Inhibition of the CDK2 and Cyclin A complex leads to autophagic degradation of CDK2 in cancer cells. *Nat Commun.* 2022; 13: 2835.
- Suski JM, Braun M, Strmiska V, Sicinski P. Targeting cell-cycle machinery in cancer. *Cancer Cell.* 2021; 39: 759-78.
- Hänggi K, Ruffell B. Cell death, therapeutics, and the immune response in cancer. *Trends Cancer.* 2023; 9: 381-96.
- Singh P, Lim B. Targeting Apoptosis in Cancer. *Curr Oncol Rep.* 2022; 24: 273-84.
- Yu L, Wei J, Liu P. Attacking the PI3K/Akt/mTOR signaling pathway for targeted therapeutic treatment in human cancer. *Semin Cancer Biol.* 2022; 85: 69-94.
- Afify SM, Oo A, Hassan G, Seno A, Seno M. How can we turn the PI3K/AKT/mTOR pathway down? Insights into inhibition and treatment of cancer. *Expert Rev Anticancer Ther.* 2021; 21: 605-19.
- Miller BW, Przepiorka D, de Claro RA, Lee K, Nie L, Simpson N, et al. FDA approval: idelalisib monotherapy for the treatment of patients with follicular lymphoma and small lymphocytic lymphoma. *Clin Cancer Res.* 2015; 21: 1525-9.
- Sun EJ, Wankell M, Palamuthusingam P, McFarlane C, Hebbard L. Targeting the PI3K/Akt/mTOR Pathway in Hepatocellular Carcinoma. *Biomedicines.* 2021; 9: 1639.